This article was downloaded by: [Institute Of Atmospheric Physics]
On: 09 December 2014, At: 15:40
Publisher: Taylor & Francis
Informa Ltd Registered in England and Wales Registered Number: 1072954 Registered office: Mortimer House, 37-41 Mortimer Street, London W1T 3JH, UK

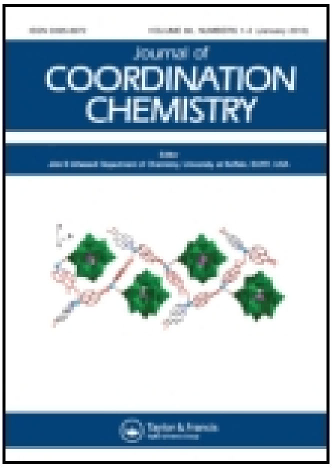

Click for updates

Journal of Coordination Chemistry
Publication details, including instructions for authors and subscription information:
http://www.tandfonline.com/loi/gcoo20

On the coordination behavior of the hmta toward zinc and cadmium cations in presence of sulfate(VI) and nitrate(V) anions

Rafal Kruszynski[a], Tomasz Sierański[a], Marcin Świątkowski[a], Marta Zielak[a], Jakub Wojciechowski[a], Magdalena Dzierżawska[a] & Bartłomiej Lewiński[a]

[a] Institute of General and Ecological Chemistry, Lodz University of Technology, Lodz, Poland

Accepted author version posted online: 17 Apr 2014.Published online: 16 May 2014.

To cite this article: Rafal Kruszynski, Tomasz Sierański, Marcin Świątkowski, Marta Zielak, Jakub Wojciechowski, Magdalena Dzierżawska & Bartłomiej Lewiński (2014) On the coordination behavior of the hmta toward zinc and cadmium cations in presence of sulfate(VI) and nitrate(V) anions, Journal of Coordination Chemistry, 67:8, 1332-1352, DOI: 10.1080/00958972.2014.915524

To link to this article: http://dx.doi.org/10.1080/00958972.2014.915524

PLEASE SCROLL DOWN FOR ARTICLE

Taylor & Francis makes every effort to ensure the accuracy of all the information (the "Content") contained in the publications on our platform. However, Taylor & Francis, our agents, and our licensors make no representations or warranties whatsoever as to the accuracy, completeness, or suitability for any purpose of the Content. Any opinions and views expressed in this publication are the opinions and views of the authors, and are not the views of or endorsed by Taylor & Francis. The accuracy of the Content should not be relied upon and should be independently verified with primary sources of information. Taylor and Francis shall not be liable for any losses, actions, claims, proceedings, demands, costs, expenses, damages, and other liabilities whatsoever or howsoever caused arising directly or indirectly in connection with, in relation to or arising out of the use of the Content.

This article may be used for research, teaching, and private study purposes. Any substantial or systematic reproduction, redistribution, reselling, loan, sub-licensing, systematic supply, or distribution in any form to anyone is expressly forbidden. Terms &

Journal of Coordination Chemistry, 2014
Vol. 67, No. 8, 1332–1352, http://dx.doi.org/10.1080/00958972.2014.915524

On the coordination behavior of the hmta toward zinc and cadmium cations in presence of sulfate(VI) and nitrate(V) anions

RAFAL KRUSZYNSKI*, TOMASZ SIERAŃSKI, MARCIN ŚWIĄTKOWSKI, MARTA ZIELAK, JAKUB WOJCIECHOWSKI, MAGDALENA DZIERŻAWSKA and BARTŁOMIEJ LEWIŃSKI

Institute of General and Ecological Chemistry, Lodz University of Technology, Lodz, Poland

(*Received 7 January 2014; accepted 25 March 2014*)

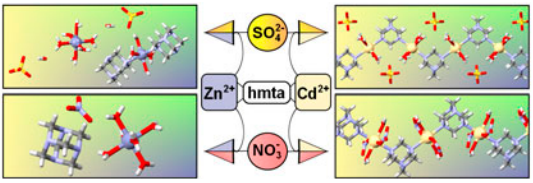

Zinc and cadmium sulfate and nitrate complexes with hexamethylenetetramine, $[Zn(hmta)_2(H_2O)_4]^{2+}\cdot[Zn(H_2O)_6]^{2+}\cdot 2SO_4^{2-}\cdot 6H_2O$ (**1**), $[Cd(hmta)(H_2O)_4]_n^{2+}\cdot nSO_4^{2-}\cdot 2nH_2O$ (**2**), $[Zn(H_2O)_6]^{2+}\cdot 2(hmta)\cdot 2NO_3^-\cdot 4H_2O$ (**3**) and $[Cd(hmta)(NO_3)_2(H_2O)_2]_n$ (**4**), have been synthesized and characterized by elemental and thermal analysis, IR spectroscopy, and X-ray crystallography.

Keywords: Zinc; Cadmium; Sulfate; Nitrate; Hexamethylenetetramine; Thermal decomposition; Spectroscopic properties

1. Introduction

Crystal engineering has developed significantly in the recent years, especially the design, synthesis, and characterization of new complexes and supramolecular architectures [1–3]. Coordination polymers are of interest for various structural topologies and intriguing frameworks, specific properties such as luminescence, magnetism, physical and chemical adsorption, nonlinear optics [4–8], and potential application in catalysis, pharmacy, separation, optoelectronics, etc. [9–12]. Such compounds are also useful precursors of nanoparticles based on metal oxides [13]. An effective method to prepare such architectures is using metal ions and specific ligands in supramolecular assembly. Generally, two groups of ligands are utilized: N-donor organic compounds possessing potential bridging abilities

---

*Corresponding author. Email: rafal.kruszynski@p.lodz.pl

(e.g. 4,4′-bipyridine, 1,4,7-triazacyclononane, 1,2,4-triazole derivatives [14–16], etc.) and multifunctional organic and inorganic anions (e.g. terephthalate, thiocyanate, malonate [17, 18], etc.). By combination of ligands, synthesis of 1-D, 2-D, and 3-D polymers is possible even if mild reaction conditions are applied [19–21]. This is especially important because energy-consuming processes (like long-term hydrothermal syntheses) have limited applicability due to economic issues.

One of the most popular ligands explored during almost a half of century is hexamethylenetetraamine (hmta), with an enormous number of coordination compounds described [22]. The hmta is a strong bulky organic base good soluble in water [23]. This ligand possesses four nitrogen atoms, and hence, as a potentially tetradentate ligand, can create from one to four metal–ligand bonds [24]. These features allow construction of coordination polymers of very different dimensionality [25]. Moreover, hmta can accept hydrogen bonds, allowing construction of versatile supramolecular arrays [26]. The hmta located in the outer coordination sphere, as an effective hydrogen bond donor, can be employed to modulate inner coordination sphere composition and geometry [27]. This ligand is also used as a cross-linking agent in construction of multinuclear coordination polymers [28]. There are reported compounds containing hmta with almost every metal ion, from alkali [29] and alkaline earth metals [30], heavy metals [31, 32] and precious metals [33, 34] to rare earth metals [35, 36].

Zinc- and cadmium-based polymers draw much attention and have been widely explored [37–40]. Zinc is an essential element for all living organisms and its coordination compounds control the proper functioning of certain enzymes [41], detect phosphoprotein, and also supply phosphopeptides and other phosphate derivatives intracellularly [42]. Metal-organic compounds containing Zn(II) coordination centers can be used as pH sensors, luminescent materials [43, 44], and biosensors. Additionally, some coordination compounds of zinc have antioxidant properties and are also used as antiulcer drugs [45]. Cadmium always accompanies zinc in natural sources and is a by-product of zinc metallurgy. Biological role of cadmium is not known yet, but its ions are important in biochemical sciences, e.g. in preparation of protein crystals [46]. Coordination polymers of cadmium are important due to their optical and luminescent properties, clathration, molecular magnetism [47, 48], etc. and they are used in many industrial fields including gas storage and separation processes [49]. In addition, supramolecular structures of Cd(II) attract much attention because of their softness and a possibility to obtain Cd(II) compounds with different coordination numbers and various geometries [47, 50].

In this work, we present the syntheses, structures, spectroscopic, and thermal analysis of four coordination compounds, $[Zn(hmta)_2(H_2O)_4]^{2+}\cdot[Zn(H_2O)_6]^{2+}\cdot 2SO_4^{2-}\cdot 6H_2O$ (**1**), $[Cd(hmta)(H_2O)_4]_n^{2+}\cdot nSO_4^{2-}\cdot 2nH_2O$ (**2**), $[Zn(H_2O)_6]^{2+}\cdot 2(hmta)\cdot 2NO_3^{-}\cdot 4H_2O$ (**3**) and $[Cd(hmta)(NO_3)_2(H_2O)_2]_n$ (**4**). Compounds **3** and **4** were previously structurally determined [51–53], but to check the possibility of formation of compounds with different metal (M) to ligand (L) ratio, the syntheses were repeated with M : L equal to 1 : 1 and 1 : 2. Additionally, some properties of **3** and **4** were not studied previously.

2. Experimental setup

2.1. *Synthesis*

All reactants (except the cadmium nitrate(V)) were of analytical grade and obtained from POCh Gliwice. The solution of cadmium nitrate (containing 0.008 mol of $Cd(NO_3)_2$) was prepared by suspending cadmium oxide (0.025 mol, 3.2103 g) in 31.25 cm^3 of a standard solution of nitric(V) acid (0.016 mol HNO_3 in water, $c = 0.500$ mol dm^{-3}). The suspension was stirred on a magnetic stirrer until pH of the mixture was 7.0 (about 3 min). The mixture was filtered to remove unreacted excess of cadmium oxide. The residue on the filter was washed thrice with 5 cm^3 of cold water and all solutions were combined. The last filtrate showed no presence of nitrate ions on the basis of test with brucine in concentrated sulfuric(VI) acid.

Solutions of respective salts (zinc sulfate(VI) heptahydrate, 0.001 mol, 0.2875 g in 5 cm^3 of water; cadmium sulfate(VI) octahydrate, 0.001 mol of Cd^{2+} ions, 0.2565 g in 5 cm^3 of water; zinc nitrate(V) hexahydrate 0.001 mol, 0.2975 g in 4 cm^3 of water) were mixed with solutions of hexamethylenetetramine (hmta, 0.001 mol, 0.1402 g in 7 cm^3 of water). The above-described solutions of cadmium nitrate(V) were also mixed with solution of hmta (0.008 mol, 1.1215 g in 8 cm^3 of water).

To determine the influence of metal : ligand reaction stoichiometry on the final product, all syntheses were repeated with doubled amounts of hmta (0.002 mol, 0.2804 g in 10 cm^3 of water and 0.016 mol, 2.2432 g in 16 cm^3 of water, respectively). In all cases, after two weeks, colorless crystals were obtained and separated from the solution by filtration on the small Buchner funnel. Elemental analyses for compounds were the same within experimental error for both L : M stoichiometries used in syntheses and mean values of three determinations for 1 : 1 L : M ratio were [Calculated/Found (%)]: (**1**) $C_{12}H_{56}N_8O_{24}S_2Zn_2$ C 16.17/16.20; H 6.33/6.28; N 12.57/12.60; O 43.07/42.98; S 7.19/7.08; Zn 14.67/14.44; (**2**) $C_6H_{24}CdN_4O_{10}S$ C 15.78/15.58; H 5.30/5.34; N 12.27/12.07; O 35.03/34.95; S 7.02/7.08; Cd 24.61/24.45; (**3**) $C_{12}H_{44}N_{10}O_{16}Zn$ C 22.18/22.16; H 6.82/6.80; N 21.55/21.48; O 39.39/39.19; Zn 10.06/9.08; (**4**) $C_6H_{16}CdN_6O_8$ C 17.46/17.26; H 3.91/4.00; N 20.37/20.51; O 31.02/31.00; Cd 27.24/27.04. The determined densities were: 1.63, 1.91, 1.55, and 2.09 g cm^{-3}, respectively for **1**, **2**, **3**, and **4**.

2.2. *Crystal structure determination*

Colorless rectangular prism-shaped crystals were mounted on a KM-4-CCD automatic diffractometer equipped with a CCD detector, and used for data collection. X-ray intensity data were collected with graphite-monochromated Mo K_α radiation ($\lambda = 0.71073$ Å) at 291.0 (3) K, with ω scan mode. Ten second exposure time was used for each compound, and all reflections inside the Ewald sphere were collected up to $\theta = 25°$ for **1–3** and up to $\theta = 36°$ for **4** (due to C centering, the set of reflections collected to smaller θ angle has unacceptable reflection to parameter ratio). The unit cell parameters were determined from least-squares refinement of the 6847, 8005, 2939, and 2774 strongest reflections, respectively, for **1–4**. Details concerning crystal data and refinement are given in table 1. Examination of reflections on two reference frames monitored after each 20 frames measured showed 2.52, 0.75, and 1.12 loss of intensity for **1**, **2**, and **3**, respectively, and no loss of the intensity for **4**. Lorentz, polarization, decay, and numerical absorption [54] corrections were applied. The structures were solved by direct methods. All nonhydrogen atoms were refined anisotropically using full-matrix, least-squares method on F^2. All hydrogen atoms were found on the difference Fourier syntheses and were refined in riding model. The isotropic displacement factors of hydrogen atoms were equal 1.2 and 1.5 times the value of equivalent displacement factor of the patent carbon and oxygen atoms, respectively The carbon-bonded hydrogen atom positions were idealized after each cycle of refinement. The SHELXS97 [55],

Table 1. Crystal data and structure refinement details for **1**–**4**.

Compound	**1**	**2**	**3**	**4**
Empirical formula	$C_{12}H_{56}N_8O_{24}S_2Zn_2$	$C_6H_{24}CdN_4O_{10}S$	$C_{12}H_{44}N_{10}O_{16}Zn$	$C_6H_{16}CdN_6O_8$
Formula weight	891.51	456.75	649.94	412.65
Crystal system, space group	Triclinic, *P*-1 (No. 2)	Triclinic, *P*-1 (No. 2)	Triclinic, *P*-1 (No. 2)	Monoclinic, *C2/c* (No. 15)
Temperature [K]	291.0(3)	291.0(3)	291.0(3)	291.0(3)
Unit cell dimensions [Å, °]	$a = 9.2554(3)$	$a = 11.2012(8)$	$a = 9.0792(2)$	$a = 8.8417(3)$
	$b = 13.3756(5)$	$b = 12.2477(8)$	$b = 9.3656(3)$	$b = 12.1135(4)$
	$c = 16.0848(8)$	$c = 12.7295(10)$	$c = 9.6835(2)$	$c = 12.9361(5)$
	$\alpha = 65.505(4)$	$\alpha = 72.127(11)$	$\alpha = 88.065(2)$	$\alpha = 90.00$
	$\beta = 89.762(4)$	$\beta = 72.683(8)$	$\beta = 75.547(2)$	$\beta = 109.161(4)$
	$\gamma = 89.686(3)$	$\gamma = 82.724(9)$	$\gamma = 61.556(3)$	$\gamma = 90.00$
Volume [$Å^3$]	1811.99(13)	1585.5(2)	697.59(3)	1308.75(8)
Z, Calculated density [$Mg\,m^{-3}$]	2, 1.634	4, 1.913	1, 1.547	4, 2.094
Absorption coefficient [mm^{-1}]	1.534	1.564	0.966	1.723
F (0 0 0)	936	928	344	824
Crystal size [mm]	0.194 × 0.157 × 0.142	0.098 × 0.086 × 0.082	0.291 × 0.218 × 0.205	0.019 × 0.017 × 0.010
θ Range for data collection [°]	1.67–25.02	1.75–25.02	2.26–25.02	2.96–35.98
Index ranges	$-11 \le h \le 9$, $-15 \le k \le 15$, $-19 \le l \le 18$	$-13 \le h \le 13$, $-14 \le k \le 14$, $-15 \le l \le 15$	$-10 \le h \le 10$, $-11 \le k \le 10$, $-11 \le l \le 10$	$-14 \le h \le 10$, $-20 \le k \le 20$, $-15 \le l \le 21$
Reflections collected/unique	18,462/6378 [$R_{(int)} = 0.0331$]	21,888/5561 [$R_{(int)} = 0.0216$]	7026/2468 [$R_{(int)} = 0.0227$]	10,544/3104 [$R_{(int)} = 0.0182$]
Completeness to $\theta = 25°$ [%]	99.9	99.3	100	100
Min. and max. transmission	0.754 and 0.797	0.863 and 0.876	0.782 and 0.819	0.965 and 0.987
Data/restraints/parameters	6378/0/439	5561/0/403	2468/0/178	3104/0/118
Goodness-of-fit on F^2	1.042	1.174	1.140	1.081
Final *R* indices [$I > 2\sigma(I)$]	$R_1 = 0.0608$, $wR_2 = 0.1916$	$R_1 = 0.0479$, $wR_2 = 0.1500$	$R_1 = 0.0293$, $wR_2 = 0.0849$	$R_1 = 0.0141$, $wR_2 = 0.0383$
R indices (all data)	$R_1 = 0.0792$, $wR_2 = 0.2011$	$R_1 = 0.0514$, $wR_2 = 0.1506$	$R_1 = 0.0324$, $wR_2 = 0.0888$	$R_1 = 0.0162$, $wR_2 = 0.0391$
Largest diff. peak and hole [$e\,Å^{-3}$]	0.911 and −0.810	1.222 and −0.840	0.713 and −0.409	0.220 and −0.374

Table 2. Selected structural data of **1–4** [Å, °, valence units].

i–j	d_{ij}	v_{ij}	i–j–k	α_{ijk}
Compound **1**				
Zn1–O1	2.091(3)	0.343	O2–Zn1–O1	86.46(12)
Zn1–O2	2.080(3)	0.353	O2–Zn1–O1^{i}	93.54(12)
Zn1–O3	2.098(3)	0.336	O2–Zn1–O3	93.56(12)
			O2–Zn1–O3^{i}	86.44(12)
			O1–Zn1–O3	86.29(13)
			O1–Zn1–O3^{i}	93.71(13)
Zn2–O4	2.098(3)	0.336	O6–Zn2–O5	86.57(12)
Zn2–O5	2.084(3)	0.349	O6–Zn2–O5^{ii}	93.43(12)
Zn2–O6	2.082(3)	0.351	O6–Zn2–O4	86.60(12)
			O6–Zn2–O4^{ii}	93.40(12)
			O5–Zn2–O4	93.64(12)
			O5–Zn2–O4^{ii}	86.36(12)
Zn3–N1	2.399(4)	0.177	O8–Zn3–O7	92.35(14)
Zn3–O7	2.044(3)	0.389	O8–Zn3–O7^{iii}	87.65(14)
Zn3–O8	2.034(3)	0.400	O8–Zn3–N1	90.29(13)
			O8–Zn3–N1^{iii}	89.71(13)
			O7–Zn3–N1	92.47(13)
			O7–Zn3–N1^{iii}	87.53(13)
Zn4–N5	2.385(4)	0.184	O10–Zn4–O9	93.16(15)
Zn4–O9	2.046(3)	0.387	O10–Zn4–O9^{iv}	86.84(15)
Zn4–O10	2.034(3)	0.400	O10–Zn4–N5	87.78(14)
			O10–Zn4–N5^{iv}	92.22(14)
			O9–Zn4–N5	89.84(14)
			O9–Zn4–N5^{iv}	90.16(14)
Compound **2**				
Cd1–N1	2.445(7)	0.337	O2–Cd1–O1	89.5(2)
Cd1–O1	2.318(6)	0.308	O2–Cd1–O1^{iii}	90.5(2)
Cd1–O2	2.257(6)	0.363	O2–Cd1–N1	87.2(2)
			O2–Cd1–N1^{iii}	92.8(2)
			O1–Cd1–N1	88.1(2)
			O1–Cd1–N1^{iii}	91.9(2)
Cd2–N2	2.440(7)	0.342	O3–Cd2–O4	88.0(2)
Cd2–O3	2.257(6)	0.363	O3–Cd2–O4^{i}	92.0(2)
Cd2–O4	2.304(6)	0.319	O3–Cd2–N2	86.4(2)
			O3–Cd2–N2^{i}	93.6(2)
			O4–Cd2–N2	89.9(2)
			O4–Cd2–N2^{i}	90.1(2)
Cd11–N11	2.396(7)	0.385	O11–Cd11–O12	89.9(2)
Cd11–O11	2.281(6)	0.340	O11–Cd11–O12^{ii}	90.1(2)
Cd11–O12	2.297(6)	0.326	O11–Cd11–N11	89.6(2)
			O11–Cd11–N11^{ii}	90.4(2)
			O12–Cd11–N11	88.9(2)
			O12–Cd11–N11^{ii}	91.1(2)
Cd12–N12	2.406(7)	0.375	O13–Cd12–O14	89.3(2)
Cd12–O13	2.259(6)	0.361	O13–Cd12–O14^{iv}	90.7(2)
Cd12–O14	2.293(6)	0.329	O13–Cd12–N12	86.5(2)
			O13–Cd12–N12^{iv}	93.5(2)
			O14–Cd12–N12	89.5(2)
			O14–Cd12–N12^{iv}	90.5(2)
Compound **3**				
Zn1–O1	2.1009(14)	0.334	O2–Zn1–O1	91.37(6)
Zn1–O2	2.0337(13)	0.400	O2–Zn1–O1^{v}	88.63(6)
Zn1–O3	2.1029(13)	0.332	O2–Zn1–O3	87.63(6)
			O2–Zn1–O3^{v}	92.37(6)

(*Continued*)

Table 2. (*Continued*).

i–*j*	d_{ij}	v_{ij}	*i*–*j*–*k*	α_{ijk}
			O1–Zn1–O3	87.21(6)
			O1–Zn1–O3^{v}	92.79(6)
Compound **4**				
Cd1–N1	2.4079(13)	0.373	O4–Cd1–O1	101.42(5)
Cd1–O1	2.3113(17)	0.313	O4–Cd1–O1^{vi}	78.58(5)
Cd1–O4	2.2829(12)	0.338	O4–Cd1–N1	90.90(4)
			O4–Cd1–N1^{vi}	89.10(4)
			O1–Cd1–N1	88.52(6)
			O1–Cd1–N1^{vi}	91.48(6)

Note: Symmetry transformations used to generate equivalent atoms: (i) $-x+2$, $-y$, $-z+1$; (ii) $-x+1$, $-y+1$, $-z$; (iii) $-x+2$, $-y$, $-z$; (iv) $-x+1$, $-y+1$, $-z+1$; (v) $-x$, $-y$, $-z+2$; and (vi) $-x+1.5$, $-y+0.5$, $-z+1$.

SHELXL97 [56], and SHELXTL [57] programs were used for all the calculations. Atomic scattering factors were those incorporated in the computer programs. Selected structural data are given in tables 2 and 3.

2.3. *Other measurements*

Elemental analyses were carried out using a Vario EL III CHNOS Elemental Analyzer (C, H, N, O, S). Zinc(II) and cadmium(II) contents were determined by complexometric titration with EDTA (0.01 mol dm^{-3} water solution) [58]. IR spectra of the samples as KBr pellets were recorded on a Jasco FT/IR 6200 spectrophotometer from 4000 to 400 cm^{-1}. The TG-MS system, used to monitor volatile products produced during thermal decomposition or fragmentation, consisted of a TG/DTA (SETSYS-16/18) coupled to a mass spectrometer (QMS-422; ThermoStar Balzers Instruments) with a platinum crucible 100 mm^3. The heating rate was 2 °C min^{-1}. Dynamic measurements were carried out in air at a flow rate of 1 dm^3 h^{-1}. Sample masses were 10.04, 10.54, 9.18, and 9.95 mg, respectively, for **1**, **2**, **3**, and **4**. An ion source had temperature of 423 K obtained by using 70 eV electron impact ionization. The solid products of thermal decomposition were determined from thermoanalytical curves [59] and on the basis of IR spectra and elemental analyses of the sinters. The final and some transition products of decomposition were confirmed by X-ray powder diffraction (XRPD) using the powder diffraction file [60] or literature data. The XRPD patterns were measured in reflection mode on an XPert PRO XRPD system equipped with a Bragg–Brentano PW 3050/65 high-resolution goniometer and PW 3011/20 proportional point detector. Cu $K\alpha_1$ radiation was used. The patterns were measured at 291.0(2) K from 2° to 90° with the narrowest beam attenuator. A diamond powder was used as an internal reference. The samples were sprinkled onto the sample holders using a small sieve, to avoid a preferred orientation. The thicknesses of the samples were no more than 0.1 mm. During the measurements, each specimen was spun in the specimen plane to improve particle statistics. The compounds density was determined in benzene by a Berman density torsion balance.

3. Results and discussion

The hmta acting as a ligand most often creates 2 : 1 L : M stoichiometry in the solid state [61], regardless of the stoichiometry used in synthesis. Because, in known compounds

Table 3. Hydrogen bonds in the studied compounds [Å, °].

D–H···A	d(D–H)	d(H···A)	d(D···A)	<(DHA)
Compound **1**				
O1–H1P···O99^{i}	0.86	1.82	2.683(5)	176.0
O1–H1O···N7	0.85	2.04	2.875(5)	169.0
O2–H2P···O95^{ii}	0.87	1.79	2.660(5)	174.0
O2–H2O···N2	0.89	2.00	2.873(5)	165.3
O3–H3O···N6^{iii}	0.83	2.04	2.856(5)	169.0
O3–H3P···O94^{iv}	0.87	1.84	2.701(5)	168.5
O4–H4O···N8	0.81	2.07	2.858(5)	164.2
O4–H4P···O96	0.84	1.87	2.705(5)	171.9
O5–H5O···N3^{v}	0.80	2.07	2.874(5)	173.7
O5–H5P···O97	0.89	1.78	2.667(5)	173.7
O6–H6O···N4	0.82	2.03	2.844(5)	167.8
O6–H6P···O98	0.87	1.81	2.671(5)	172.2
O7–H7P···O12^{vi}	0.80	1.38	2.161(6)	162.7
O7–H7P···O13	0.80	1.90	2.699(5)	179.8
O8–H8O···O12^{i}	0.85	1.96	2.801(6)	171.2
O8–H8P···O15^{iv}	0.82	1.81	2.631(5)	173.1
O9–H9O···O17^{vii}	0.82	1.86	2.677(5)	179.4
O9–H9P···O18^{viii}	0.82	1.97	2.791(5)	179.5
O10–H10O···O14^{ix}	0.85	1.82	2.605(6)	152.1
O10–H10P···O18	0.86	2.13	2.973(6)	165.2
O94–H94O···O13^{ix}	0.81	2.11	2.909(6)	166.8
O94–H94P···O16	0.84	2.05	2.845(6)	158.2
O95–H95P···O16^{vii}	0.82	1.97	2.787(6)	179.8
O95–H95O···O14^{ix}	0.82	1.98	2.805(6)	179.9
O96–H96P···O17^{vii}	0.77	2.06	2.827(6)	172.3
O96–H96O···O11^{ix}	0.86	1.99	2.847(7)	177.0
O97–H97O···O11^{ix}	0.83	1.93	2.759(6)	176.2
O97–H97P···O15	0.82	1.95	2.772(5)	179.9
O98–H98O···O11^{vi}	0.87	1.91	2.774(6)	171.2
O98–H98P···O12	0.86	2.60	3.133(7)	121.0
O98–H98P···O13	0.86	2.15	3.011(7)	179.7
O99–H99P···O16^{viii}	0.86	1.92	2.774(6)	173.7
O99–H99O···O17^{vii}	0.85	2.55	3.270(7)	142.6
O99–H99O···O18^{vii}	0.85	2.19	2.979(6)	153.5
C1–H1B···O12^{i}	0.97	2.51	3.412(6)	154.7
C1–H1A···O94^{iv}	0.97	2.52	3.463(6)	163.4
C3–H3A···O98^{i}	0.97	2.55	3.486(6)	161.4
C3–H3A···O7^{x}	0.97	2.60	3.136(6)	115.2
C4–H4A···O96^{xi}	0.97	2.53	3.465(6)	160.6
C7–H7B···O99	0.97	2.54	3.458(6)	158.2
C9–H9A···O18	0.97	2.54	3.450(6)	155.4
C9–H9B···O95^{viii}	0.97	2.50	3.436(6)	163.1
C10–H10B···O10	0.97	2.57	3.121(6)	116.3
C10–H10B···O97	0.97	2.52	3.468(6)	164.5
Compound **2**				
O1–H1O···O21^{vii}	0.84	1.89	2.716(9)	167.9
O1–H1P···O32	0.84	1.97	2.808(9)	179.6
O2–H2O···O24^{vii}	0.81	1.89	2.687(10)	166.1
O2–H2P···O92	0.81	1.84	2.658(10)	179.6
O3–H3O···O22^{vii}	0.87	1.87	2.704(10)	158.5
O3–H3P···O91	0.82	1.82	2.643(10)	175.3
O4–H4P···O21^{vii}	0.93	1.94	2.821(10)	158.2
O4–H4P···O22^{vii}	0.93	2.58	3.302(11)	134.6
O4–H4O···O33	0.87	1.86	2.721(10)	174.9
O11–H11P···N4^{v}	0.83	2.04	2.868(9)	179.8

(*Continued*)

Table 3. (*Continued*).

D–H···A	d(D–H)	d(H···A)	d(D···A)	<(DHA)
O11–H11O···O31	0.82	1.89	2.707(9)	179.2
O12–H12O···O32	0.83	1.90	2.728(10)	176.7
O12–H12P···O93	0.84	1.89	2.722(9)	169.2
O13–H13P···O23^{xiii}	0.91	1.81	2.710(10)	169.4
O13–H13O···O33	0.84	1.89	2.716(10)	166.0
O14–H14O···O24^{xii}	0.83	1.92	2.740(10)	170.0
O14–H14P···O31	0.82	1.91	2.730(9)	179.7
O91–H91O···O33^{xiii}	0.82	2.14	2.963(12)	179.7
O91–H91P···N13^{iii}	0.89	2.01	2.780(10)	144.0
O92–H92O···O32^{x}	0.81	1.97	2.775(11)	179.8
O92–H92P···O34^{iv}	0.88	2.05	2.926(11)	179.6
O93–H93O···O21^{vii}	0.83	2.16	2.986(12)	173.4
O93–H93P···O22^{xiii}	0.87	1.98	2.822(11)	162.0
O94–H94O···N3	0.81	2.11	2.914(11)	179.7
O94–H94P···O23	0.89	2.41	3.228(12)	152.3
O94–H94P···O24	0.89	2.32	3.082(14)	144.1
C1–H1B···O3	0.97	2.55	3.215(11)	125.3
C3–H3A···N14^{ii}	0.97	2.58	3.412(12)	144.3
C5–H5A···O34	0.97	2.54	3.427(12)	151.6
C6–H6A···O93^{i}	0.97	2.44	3.395(12)	166.5
C6–H6B···O94^{xiv}	0.97	2.37	3.283(12)	157.4
C15–H15B···O94^{xii}	0.97	2.57	3.475(13)	156.1
C16–H16A···O92^{xii}	0.97	2.44	3.382(12)	163.5
C16–H16B···O91^{xii}	0.97	2.44	3.366(12)	158.8
Compound **3**				
O1–H1P···N4^{vii}	0.90	1.98	2.868(2)	171.2
O1–H1O···O11	0.85	2.02	2.858(3)	166.2
O2–H2P···O99^{iii}	0.83	1.85	2.663(2)	165.1
O2–H2O···N3	0.76	2.03	2.792(2)	177.7
O3–H3O···O12^{xv}	0.81	2.05	2.837(2)	165.9
O3–H3P···N1^{xvi}	0.79	2.05	2.820(2)	165.1
O98–H98O···O13	0.88	1.92	2.805(3)	173.9
O98–H98P···O12	0.94	2.02	2.911(3)	159.7
O98–H98P···O13^{xvii}	0.94	2.48	3.292(4)	145.5
O99–H99O···N2	0.81	2.01	2.819(2)	173.5
O99–H99P···O98	0.88	1.93	2.816(3)	175.8
C4–H4A···O99^{viii}	0.97	2.57	3.467(3)	154.6
C5–H5A···O12^{iii}	0.97	2.55	3.448(3)	153.9
Compound **4**				
O4–H4O···O3^{xiii}	0.87	2.20	3.041(6)	160.7
O4–H4P···N2^{xviii}	0.94	1.86	2.8026(18)	174.3
O4–H4O···O3	0.87	2.57	3.013(5)	112.7
C1–H1B···O3^{xiii}	0.97	2.52	3.494(4)	178.1
C1–H1A···O2^{xix}	0.97	2.53	3.383(5)	147.0
C4–H4B···O2^{xix}	0.97	2.45	3.325(5)	150.2
C4–H4B···O1^{xx}	0.97	1.85	2.231(2)	99.6

Note: Symmetry transformations used to generate equivalent atoms: (i) $x+1, y, z$; (ii) $x+1, y-1, z$; (iii) $-x+1, -y, -z+1$; (iv) $x, y-1, z$; (v) $-x+2, -y+1, -z$; (vi) $-x+1, y, z$; (vii) $x-1, y, z$; (viii) $-x-1, -y-1, -z-1$; (ix) $x, y+1, z$; (x) $-x+2, -y, -z$; (xi) $-x+1, -y+1, z$; (xii) $x-1, y+1, z$; (xiii) $-x+2, -y, -z+1$; (xiv) $-x+3, -y, -z$; (xv) $x, y, z+1$; (xvi) $-x, -y+1, -z+2$; (xvii) $-x, -y+1, -z+1$; (xviii) $x, -y, z+0.5$; (xix) $-x+2, y, -z+0.5$; and (xx) $x-0.5, -y+0.5, -z+0.5$.

containing $M(NO_3)_2$ (where M = Zn, Cd) and hmta, the Zn : hmta ratio is 1 : 2 [52] and the Cd : hmta ratio is 1 : 1 [51, 53], the syntheses were additionally performed in two complementary stoichiometries Zn : hmta 1 : 1 and Cd : hmta 1 : 2, to check the possibility of formation of compounds with different M : L ratios. Analogous experiments were performed for $M(SO_4)$ salts. In all cases, the obtained products were the same for both L : M stoichiometries used in syntheses. The identities of the solid compounds were confirmed by elemental analyses accompanied by XRPD and IR spectroscopy (elemental analysis may be inconclusive because it may give the same results in case of formed compound and mixture of the reactants with the same stoichiometry). The registered XRPD patterns and IR spectra were the same in the range of experimental error. The three compounds have the less common 1 : 1 stoichiometry (these ones containing the $M(SO_4)$ and $Zn(NO_3)_2$) and one compound has the 1 : 2 M : L ratio (this one containing $Cd(NO_3)_2$).

The synthesized compounds are air stable, soluble in water, and insoluble in benzene. As expected, the density of the cadmium coordination compounds is larger than of zinc ones (about 0.3 g cm^{-3} in case of sulfates(VI) and about 0.5 g cm^{-3} in case of nitrates(V)).

The structural investigations show that the Zn1, Zn2, Zn3, and Zn4 atoms of **1** (figure 1) occupy, respectively, the special positions *b*, *e*, *a*, and *h* of the *P*-1 space group with site symmetry −1 and multiplicity 1 [62], thus the asymmetric unit contains halves of the four complex cations (two $Zn(hmta)_2(H_2O)_4]^{2+}$ and two $[Zn(H_2O)_6]^{2+}$), two sulfate(VI) anions and four water molecules. Such composition makes **1** structurally unique because it contains two uncommon features, i.e. two different complex cations of one metal in the crystal net and two halves of each cation in the asymmetric unit (typically only one half of cation with internal symmetry exists) [61]. The Cd1, Cd2, Cd11, and Cd12 atoms of **2** (figure 2) are located, respectively, at the special positions *a*, *b*, *e*, and *h* of *P*-1 space group. As a consequence, the cations and organic ligand assemble to chains propagating along the crystallographic [0 0 1] axis, and the asymmetric unit contains the $[Cd_{0.5}(H_2O)_2(hmta)(H_2O)_2Cd_{0.5}]$ parts of two polymeric chains, two sulfate(VI) anions, and four water molecules. In both **1** and **2**, the same special positions are occupied by metal cations but the formed structures

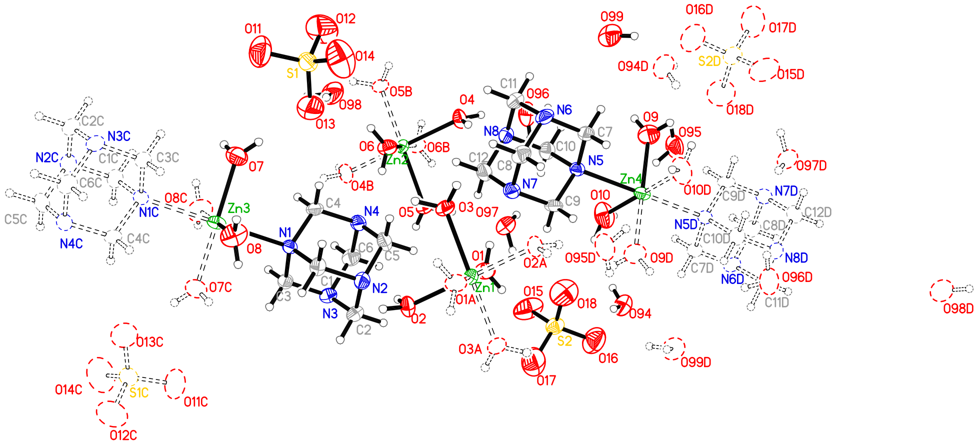

Figure 1. The solid state structure of **1** with atom numbering scheme, plotted with 50% probability of displacement ellipsoids of nonhydrogen atoms. The hydrogen atoms are plotted as spheres of arbitrary radii. The symmetry-generated atoms indicated by A, B, C, and D letters were obtained *via* $-x+2$, $-y$, $-z+1$; $-x+1$, $-y+1$, $-z$; $-x+2$, $-y$, $-z$; $-x+1$, $-y+1$, $-z+1$ symmetry transformations, respectively.

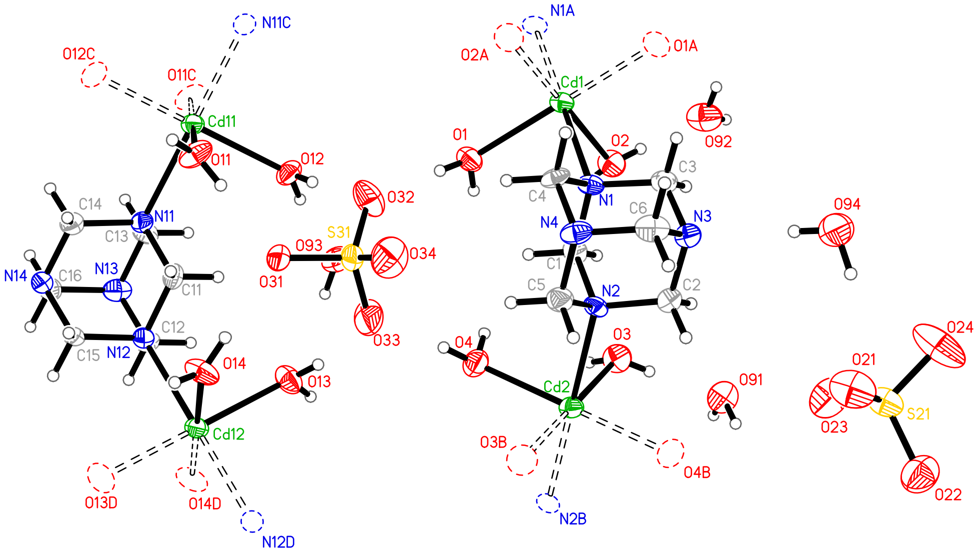

Figure 2. The solid state structure of **2** with atom numbering scheme, plotted with 50% probability of displacement ellipsoids of nonhydrogen atoms. The hydrogen atoms are plotted as spheres of arbitrary radii. The symmetry-generated atoms indicated by A, B, C, and D letters were obtained *via* $-x+2$, $-y$, $-z$; $-x+2$, $-y$, $-z+1$; $-x+1$, $-y+1$, $-z$; $-x+1$, $-y+1$, $-z+1$ symmetry transformations, respectively.

are distinctly different. The Zn1 and Cd1 atoms of **3** and **4** (figures 3 and 4) occupy, respectively, the special position *a* of the *P*-1 space group (site symmetry −1, multiplicity 1) and *d* of the *C2/c* space group (site symmetry −1, multiplicity 4). Additionally in **4**, C2 and C3 atoms of hmta molecule are located at the special position *a* of the *C*2/*c* space group (site symmetry 2, multiplicity 4). Above-mentioned symmetry operation expands the asymmetric unit of **3** to $[Zn(H_2O)_6]^{2+}$ cations and clearly separated two hmta molecules, two nitrate(V) anions, and four water molecules. The listed symmetry elements build up the asymmetry unit of **4** to $[Cd(hmta)(NO_3)_2(H_2O)_2]_n$ chain propagating along the crystallographic [10–1] axis. The central ions are six-coordinated by six water molecules (the Zn1 and Zn2 cations of **1** and Zn1 cation of **3**), or by two nitrogen atoms of two hmta molecules and four waters (the Zn3 and Zn4 cations of **1** and all Cd cations of **2**), or by two nitrogen atoms of two hmta molecules, two oxygen atoms of two nitrate(V) anions and two water molecules (the Cd cation of **4**). The coordination polyhedra of all central ions can be described as ideal (by symmetry) tetragonal bipyramids (figure 5) [63]. The bonds within sulfate(VI) anions are fully delocalized and slightly localized within nitrate(V) anions. The nitrate(V) anion of **4** shows disorder similar to the previously described one [53]. The hmta N–C bond lengths in all compounds are similar to those of pure hmta [64] and its compounds [23, 27, 30].

The bond valences were computed as $v_{ij} = \exp[(R_{ij} - d_{ij})/b]$ [65, 66], where R_{ij} is the bond-valence parameter (in the formal sense, R_{ij} can be considered as a parameter equal to the idealized single-bond length between *i* and *j* atoms for given *b*) and *b* was taken as 0.37 Å [67, 68]. The R_{Zn-O}, R_{Zn-N}, R_{Cd-O} and R_{Cd-N} were taken from literature data [38] (containing re-determined parameters for coordination compounds, as previously described [69, 70]) and their values were 1.6950, 1.7588, 1.8818, and 2.0430, respectively. The computed bond valences are collected in table 2. The computed total valences of the central

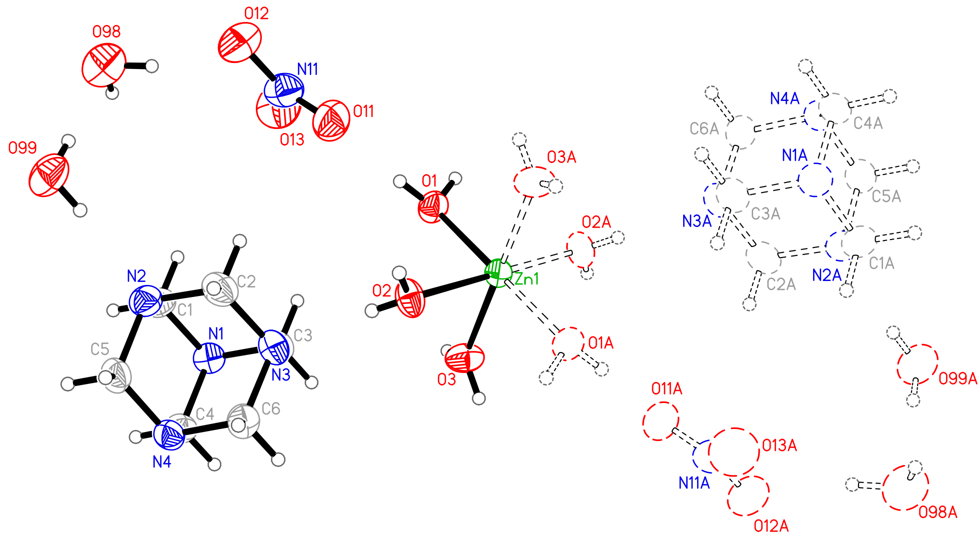

Figure 3. The solid state structure of **3** with atom numbering scheme, plotted with 50% probability of displacement ellipsoids of nonhydrogen atoms. The hydrogen atoms are plotted as spheres of arbitrary radii. The symmetry-generated atoms indicated by A letter were obtained *via* $-x$, $-y$, $-z+2$ symmetry transformations, respectively.

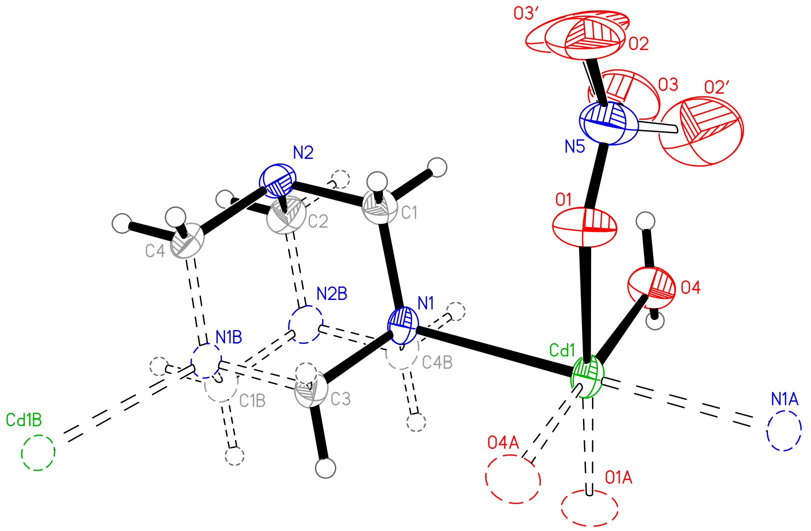

Figure 4. The solid state structure of **4** with atom numbering scheme, plotted with 50% probability of displacement ellipsoids of nonhydrogen atoms. The hydrogen atoms are plotted as spheres of arbitrary radii. The symmetry-generated atoms indicated by A and B letters were obtained *via* $-x+1.5$, $-y+0.5$, $-z+1$ and $-x+1$, y, $-z+0.5$ symmetry transformations, respectively.

ions (BVS) are very close to the expected +2 (formal oxidation state of metal), and small deviations (negative and positive in **1**, only positive in other compounds) may originate from restraints imposed by rigid polymeric chains and relatively strong intermolecular

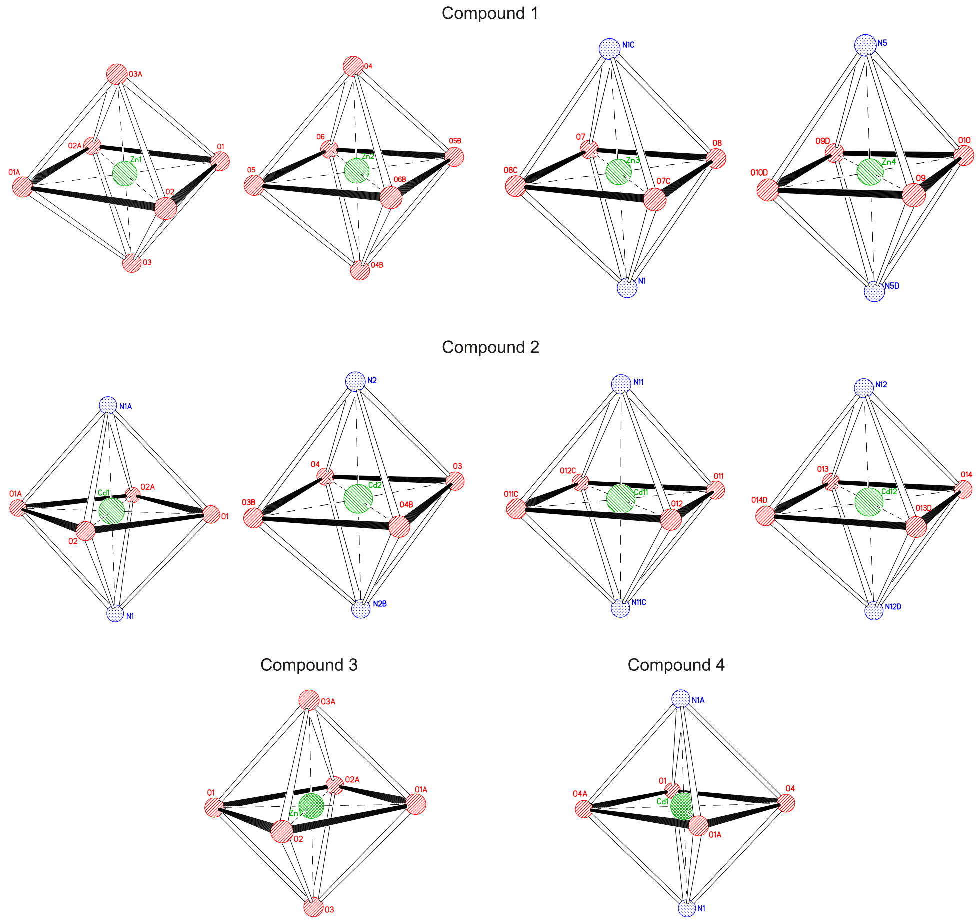

Figure 5. The coordination polyhedra in **1**–**4**.

interactions, preventing the coordination environment from attaining the most favorable geometry. Noteworthy is the fact that in **1,** the M–O coordination bonds are twice stronger than M–N bonds, while in other studied compounds M–N and M–O, coordination bonds have comparable strength. This, together with negative deviations from BVS existing only in **1**, suggests that the strains within the crystal net of **1** are the largest ones.

In the structures of the investigated compounds, multiple intermolecular O–H···O, O–H···N and C–H···O hydrogen bonds exist that create the 3-D nets (table 3). They are formed between anionic species (sulfate(VI) and nitrate(V) ions), water and hmta molecules and create diverse graphs [71–74]. Unitary graph sets of **2** and **3** consist only of D patterns. In case of **1**, only C patterns exist in the first level graph, i.e. six $C_2^2(12)$ patterns formed by O–H···N hydrogen bonds (existing between zinc coordinated water and hmta molecules). N_1 graph of **4** is more complex and it consists of $C_1^1(6)C_1^1(6)R_2^2(12)R_2^2(12)$ motifs. One C and one R pattern is created by O–H···O hydrogen bonds, while the remaining ones are formed by O–H···N hydrogen bonds. These bonds exist between water molecules and nitrate(V) ions (O–H···O) or hmta molecules (O–H···N). Binary graph sets of **1** and **2** are complicated and contain multiple multiatomic C and R patterns. In **1**, the numerous $C_4^4(16)$, $C_4^4(24)$, $R_4^4(12)$, $R_4^4(16)$, $R_4^4(24)$, and $R_6^6(32)$ patterns are created by different sets of hydrogen bonds and, for example, four different $R_4^4(16)$ patterns are formed by four different pairs of hydrogen bonds. Binary graph set of **2** includes $C_4^2(12)$, $C_4^4(16)$, $R_2^2(8)$, $R_2^1(10)$, $R_2^2(12)$, and $R_4^4(12)$ patterns. Similar to **1**, each listed pattern may be created by different pairs of hydrogen bonds (e.g. 14 different $C_4^4(16)$ patterns are formed). In **1** and **2**, hydrogen bonds link the metal coordinated water molecules with sulfate(VI) ions (O–H···O bonds) and hmta molecules (O–H···N bonds), as well as link sulfate(VI) ions with water located in the outer coordination sphere (O–H···O bonds). In **3**, the $N_2C_2^2(8)C_2^2(8)C_2^2(8)C_2^2(8)R_4^4(12)C_4^4(16)C_4^4(16)C_4^4(16)C_4^4(16)R_4^4(16)R_4^4(16)R_4^4(16)R_4^4(16)$ graph is formed on the second level. Three patterns of each $C_2^2(8)$, $C_4^4(16)$ and $R_4^4(16)$ graph type are formed by O–H···N hydrogen bonds, existing between zinc-coordinated water and hmta molecules. The other patterns involve O–H···O hydrogen bonds between zinc-coordinated water molecules and nitrate(V) ions ($C_2^2(8)$, $C_4^4(16)$ and $R_4^4(16)$ patterns), or between outer coordination sphere water molecules and nitrate(V) ions (the $R_4^4(12)$ pattern). Among studied compounds, the binary graph set of **4** is the simplest one, consisting of $C_2^2(9)$, $C_2^2(10)$, $C_2^2(12)$, $R_4^4(18)$, and $R_4^4(22)$ patterns, formed by hydrogen bonds between cadmium-coordinated water molecules and two different acceptors: nitrate(V) ions (O–H···O bonds) and hmta molecules (O–H···N bonds).

Infrared spectra are consistent with existing bonds of the formed species. The spectra of compounds containing sulfate(VI) ions (**1** and **2**) exhibit characteristic bands of SO_4^{2-} (i.e. the bending vibrations at about 619 cm^{-1} (table 4) and the asymmetric stretching vibrations of tetrahedral sulfate(VI) ion at about 1051, 1112, and 1190 cm^{-1}, partially overlapped with CN stretching vibrations of hmta molecules (table 4). The last two bands in spectra of respective pure metal sulfates(VI) are observed as a single band (table 4) and its duplication in **1** and **2** is associated with the multifurcating of sulfate(VI) oxygen atoms acting as hydrogen bond acceptors. The spectrum of **1** possesses also a strong band at 990 cm^{-1} which is absent in the spectrum of **2**. This band originates from symmetric vibrations of S–O oscillators. The absence of these frequencies in **2** can be explained by more symmetrical environment of SO_4^{2-} (the hydrogen bonds formed by each specific oxygen atoms are more similar than in **1**), causing greater degeneration of the present oscillator energy levels. Spectra of compounds containing nitrate(V) groups (**3** and **4**) contain bands characteristic for NO_3^- vibrations, assigned to NO_3^- out of plane bending vibrations at 817–824 cm^{-1} and to NO_3^- asymmetric stretching vibrations at 1385 cm^{-1} (strong sharp band). The bands at 820 cm^{-1} are red shifted in comparison to the one of a free nitrate(V) ion and blue shifted in comparison to anhydrous zinc nitrate(V). This is caused by the presence of different hydrogen bonds between nitrate(V) ions and neighboring species in these structurally dissimilar compounds. The band at 1385 cm^{-1} is slightly blue shifted in comparison to free nitrate(V) ion and pure salts (table 4). The higher excitation energy of the oscillators corresponding to NO_3^- stretching vibrations is due to immobilization of these ions in the crystal nets of **3** and **4**. Some NO_3^- ion bending vibrations present in **3** are absent (at 763 cm^{-1}) or significantly weakened (777–782 cm^{-1}) in spectrum of **4**. This is caused by existence of the nitrate(V) ions of **4** in the inner coordination sphere, blocking some oscillations and diminishing the population of some NO_3^- ion oscillators. In the IR spectrum of **3,** NO_3^- combination bands and overtones are more populated than in **4** (table 4). This is caused, as above, by stabilization of nitrate(V) ions of **4** in the crystal net by coordination and hydrogen bonds (in **4,** the nitrate(V) ions form O–H···O bonds only with water molecules directly coordinated, while in **3**, the NO_3^- ions are bonded by O–H···O also with water molecules

Table 4. Vibrational frequencies [cm^{-1}] and their assignments for **1**–**4**.

1	**2**	**3**	**4**	Hmta [80, 81]	Zinc sulfate(VI) heptahydrate [82]	Cadmium sulfate (VI) octahydrate [83]	Zinc nitrate(V) (anhydrous) [84, 85]	Cadmium nitrate (V) (anhydrous) [84]	Free sulfate(VI) ion [86]	Free nitrate(V) ion [86]	Assignment
3566bb	3502bb	3502bb	3504bb								υ O–H (H_2O)
3224 m											υ O–H (H_2O)
2979vw											υ CH
2965vw	2962vw	2961w	2962w	2966							υ CH
2939vw	2935vw	2928w	2935w	2955							υ CH
2893vw	2884vw	2885w	2886w	2874							υ CH
	2074w					2078					υ CN, υ CNC deformation, *O–H ·(H_2O)
	1943vw										*O–H·(H_2O)
	1923vw										*O–H·(H_2O)
1869vw	1868vw	1868vw									υ CN
1844vw	1845vw					1838					υ CN, υ SO
		1830vw						1828			*NO_3^-
		1792vw	1788w				1802				*NO_3^-
		1772vw	1768w								*NO_3^-
		1762w									*NO_3^-
		1734vw									*NO_3^-
		1697vw									δ O–H (H_2O)
		1653w									δ O–H (H_2O)
1641s		1636w									δ O–H (H_2O)
	1624s	1617w	1624 m								δ O–H (H_2O)
	1577vw										υ CN
1559vw	1559vw	1559w									υ CN
1541w	1541w	1541w									υ CN
1522vw	1522w	1522w									υ CN
1507w	1508w	1507w									υ CN
1498vw		1497vw									υ CN, CNC deformation
1489vw	1489w					1497					υ CN, CNC deformation, υ SO
1466s	1467s	1460s	1466w	1456							σ CH_2

(*Continued*)

Table 4. (*Continued*).

1	**2**	**3**	**4**	Hmta [80, 81]	Zinc sulfate(VI) heptahydrate [82]	Cadmium sulfate (VI) octahydrate [83]	Zinc nitrate(V) (anhydrous) [84, 85]	Cadmium nitrate (V) (anhydrous) [84]	Free sulfate(VI) ion [86]	Free nitrate(V) ion [86]	Assignment
1437w	1437w			1440							σ CH$_2$
1418w	1419vw										σ CH$_2$
1397w											
				1393							CNC deformation
		1385vs	1385vs				1359	1381		1350	υ_{as} NO$_3$
1386w	1381 m			1370							τ CH$_2$
1363vw	1351vw			1346							ω CH$_2$
1340w	1332vw										ω CH$_2$
1315w	1316w										υ CN
		1256vs									υ CN
1243 m			1238s								υ CN
1231 m	1238s	1231vs		1234							υ CN
1223 m											υ CN
		1202w	1207w								υ CN, CNC deformation
1190s	1192s			1191							υ CN, CNC deformation, υ_{as} SO
1112vs	1112vs				1090	1137			1104		υ_{as} SO
		1111w									υ CN
		1059s					1040 & 1050				υ (NO$_3^-$)
1051w	1051w					1074					υ CN, υ_{as} SO
			1043w								υ CN
1024vs		1024vs		1026							υ CN
1001s	1007vs	1001vs	1006vs	1007							υ CN
990s					984				981		υ_s SO
927s	935w	934vw	931w	925							υ NC
		908 m									δ (NO$_3^-$)
		901s									δ (NO$_3^-$)
830w											υ NC
821 m	814s			825							υ NC
		824s	817s				793 & 800			830	υ NC, γ (NO$_3^-$)
803 m											υ NC
786 m	779w			779							υ NC
		777 m	782w	779				802 & 805			υ NC, γ (NO$_3^-$)

		763s					763			δ (NO_3^-)
730s					758					υ CN, O–H (H_2O) libration [87]
719vw										υ CN, O–H (H_2O) libration [87]
		714s					746		680	δ (NO_3^-)
700 m	694s	681w	695s	675						δ N–C–N, (H_2O) libration [87]
678 m	669w	662s								δ N–C–N, (H_2O) libration [87]
664w										δ N–C–N
		620w								ω O–H (H_2O), ρ O–H (H_2O)
619vs	619s				611	653		613		δ SO

Note: Vibrations symbols: vw – very weak, w – weak, m – medium strength, s – strong, vs – very strong, bb – broadened, υ – stretching, δ – bending, τ – wagging, ω – twisting, ρ – rocking, σ – scissoring, s – symmetric, as- asymmetric, * – overtone and combination band.

located in the outer coordination sphere). The hmta molecules exhibit vibrations typical for its oscillators (table 4) and most of the corresponding bands (e.g. 681–700 and 1381–1386 cm^{-1}) are shifted to higher frequencies, compared to free ligand (table 4). These shifts are caused by O–H···N and C–H···O hydrogen bonds existing between hmta molecules and other molecular and ionic species (table 3). In all spectra, the bands characteristic for stretching vibration of O–H groups are present (in the range of 1624–1697 cm^{-1} and at about 3500 cm^{-1} as strongly broadened band) (table 4).

The thermal decomposition of the compounds is a gradual process (scheme 1). Thermal analyses were previously reported for **3** (in static air, with heating rate 5 °C/min) [52] and **4** (in flowing nitrogen, with heating rate 10 °C/min) [51], but essential differences exist between the results reported in this work and those presented earlier. In all cases, the first step of decomposition is removal of water molecules. For **1**, **2**, and **3**, it starts at 30–58 °C. The exception is **4**, which is the uncommonly thermally stable (for a compound containing water molecules), and it starts decomposing at 168 °C, consistently with the previous study [51]. The dehydration of **1** and **3** (zinc compounds) is a multistep process and finishes at 184 and 193 °C, respectively. This is different from previously described thermal degradation process of **3** [52], in which this compound decomposes in two steps, losing four water molecules in the first (finished at 100 °C) and evolving remaining water molecules simultaneously with the decomposition of hmta molecules in the second step (600–645 °C). Existence of water in coordination compound at 600 °C is highly improbable. In our experiment, dehydration of **3** takes place in three steps and finishes at 193 °C. The removal of water molecules from cadmium compounds (**2** and **4**) occurs in a one-step process (scheme 1). In the previously reported study, dehydration of **4** [51] is also one step, but finished at 300 °C, opposite to the current findings (the determined end of dehydration of **4** is at 201 °C). The observed difference might originate from faster heating rate used previously (10 °C min^{-1} instead of 5 °C min^{-1}), preventing evaporation of all water molecules at lower temperature, due to providing lower amount of energy at the same time (in both cases energy required to water releasing is the same). For all compounds, dehydration is endothermic and rather quick process. Further decomposition (occurring as the temperature rises) is associated with hmta removal and the decomposition of the remaining salt (metal sulfate(VI) or nitrate(V)). The decomposition of salt and hmta molecules are overlapping exothermic processes with individual steps difficult to distinguish. For **1** and **2**, after combustion of hmta, the formed salts decompose partially to mixture of metal oxide and the metal sulfate(VI) (scheme 1). The decomposition products of **1** are stable to 850 °C, and further heating leads to slow conversion of the zinc sulfate(VI) to zinc oxide. This phenomenon was observed earlier for pure salt, i.e. zinc sulfate(VI) decomposes to mixture of zinc oxide and zinc sulfate(VI) (with the molar ratio 1 : 2) and that mixture undergoes further decomposition to zinc oxide when the temperature reaches 861 °C [75]. The decomposition products of **2** are stable to the highest measured temperature (1000 °C). The pure anhydrous cadmium sulfate(VI) is thermally stable and its m.p. is 1000 °C [76], but in **2**, the formation of cadmium oxide together with cadmium sulfate(VI) is observed. This is caused by the kinetic effects of the formation process of cadmium sulfate(VI) from sulfate(VI) ions located in the outer coordination sphere. The combustion of the hmta molecules directly bonded to the metal cation partially inhibit formation of cadmium sulfate(VI) by preceding oxidation of the cadmium (part of the outer coordination sphere sulfate(VI) ions decompose to sulfur trioxide). Analogous processes occur also in **1**. During the thermal decomposition of pure zinc sulfate(VI), mixture of zinc oxide and zinc sulfate(VI) is formed at 780 °C [75], while **1** decomposes to this mixture at 697 °C (scheme 1). Further thermal

$[Zn(hmta)_2(H_2O)_4]^{2+}\bullet[Zn(H_2O)_6]^{2+}\bullet 2SO_4^{2-}\bullet 6H_2O$
| stage I; m. l. 29.15% / 28.27%
↓ $-14H_2O$ (37-115°C) 88°C endo
$[Zn(hmta)_2(H_2O)_2]^{2+}\bullet ZnSO_4\bullet SO_4^{2-}$
| stage II; m. l. 4.99% / 4.04%
↓ $-2H_2O$ (115-184°C) endo
$[Zn(hmta)_2]^{2+}\bullet ZnSO_4\bullet SO_4^{2-}$
| stage III; m. l. 41.42% / 40.43%
↓ -2hmta (184-697°C) 697°C exo
0.67 ZnO* •1.33 $ZnSO_4$*

$[Cd(hmta)(H_2O)_4]^{2+}\bullet SO_4^{2-}\bullet 2H_2O$
| stage I; m. l. 22.53% / 23.65%
↓ $-6H_2O$ (58-168°C) 120°C endo
$[Cd(hmta)]^{2+}\bullet SO_4^{2-}$
| stage III, m.l. 43.47% /42.97 %
| stage IIIa, m.l. 12.82%/—; (168-291°C) 243°C exo
| stage IIIb, m.l. 30.65% / —; (291-627°C) 571°C exo, 617°C exo
↓ -hmta, $-0.7SO_3$,
0.7CdO*•0.3$CdSO_4$*

$[Zn(H_2O)_6]^{2+}\bullet 2(hmta)\bullet 2NO_3^-\bullet 4H_2O$
| stage I; m. l. 18.17% / 19.39%
↓ $-7H_2O$ (30-103°C) 81°C endo
$[Zn(H_2O)_3]^{2+}\bullet 2(hmta)\bullet 2NO_3^-$
| stage II; m. l. 3.15% / 2.77%
↓ $-H_2O$ (103-139°C) 131°C endo
$[Zn(H_2O)_2]^{2+}\bullet 2(hmta)\bullet 2NO_3^-$
| stage III; m. l. 4.95% / 5.54%
↓ $-2H_2O$ (139-193°C) 172°C endo
$Zn(NO_3)_2$*•2hmta*
| stage IV; m. l. 59.57% / 59.78%
| stage IVa, m.l. 30.95%/—; (193-371°C) 196°C exo, 204°C exo, 263°C exo, 338°C exo
| stage IVb, m.l. 22.62% / —; (371-573°C) 538°C exo
↓ $-2NO_2$, $-0.5O_2$, -2hmta
ZnO*

$2[Cd(hmta)(NO_3)_2(H_2O)_2]$
| stage I; m. l. 10.37% / 8.73%
| $-2H_2O$ (168-201°C) 191°C endo
$[Cd(hmta)(NO_3)_2]$
| stage II; m. l. 79.16% / 81.93%
↓ $-0.7Cd(NO_3)_2$, $-0.6NO_2$, $-0.3O_2$, -hmta (201-482°C) 258°C exo
0.3CdO*

Scheme 1. The stages of thermal decomposition of **1**–**4** (m.l. – experimental mass loss/theoretical mass loss, * – product confirmed by XRPD).

decomposition of anhydrous **3** and **4** differs from processes observed for **1** and **2**. The nitrate(V) salts (formed as intermediates during hmta removal) decompose to the metal oxide, giving nitrogen oxide and oxygen as gaseous products, according to the following equation: $2\,M(NO_3)_2 \rightarrow 2MO + 4NO_2 + O_2$ (where M = Cd, Zn) [77–79]. In **3**, this melted salt is gradually formed and it decomposes instantly after formation (m.p. of zinc nitrate(V) hexahydrate is 36 °C, of anhydrous zinc nitrate(V) is 100 °C, and anhydrous salt decomposes at about 125 °C [78, 79]). The hmta removal in **4** is a rapid process and the formed salt is partially evaporated (the anhydrous cadmium nitrate(V) m.p. is 401 °C and above this temperature, the salt evaporation begins [77]). The final decomposition products of **3** and **4** are zinc oxide and cadmium oxide, respectively (scheme 1).

4. Conclusions

The reaction of hmta with zinc and cadmium nitrates(V) as well as zinc and cadmium sulfates(VI) leads to formation of diverse coordination compounds. The electronic properties of the anions influence strongly coordination modes of hmta. The presence of sulfate(VI) anions leads to complication of the formed structures in comparison to compounds containing nitrate(V) anions. The exchange of nitrate(V) ion to sulfate(VI) ions in zinc compounds leads to formation of heteroligand $[Zn(hmta)_2(H_2O)_4]^{2+}$ instead of sole creation of simple $[Zn(H_2O)_6]^{2+}$, and in cadmium compounds to polymeric chains possessing four structurally unequal cadmium cations instead of the cadmium cations occupying the one structural site. In both cadmium compounds, hmta molecules are directly bonded to the metal cation and as bridging ligands lead to creation of polymeric species. Polymerization does not occur in the zinc compounds due to smaller stability of $Zn(hmta)_2{}^{2+}$ than $Cd(hmta)_2{}^{2+}$. The sulfate (VI) anions in both compounds are located in the outer coordination sphere, while the location of the nitrate(V) anions depends on the cation electronic properties, for more electronegative cadmium, they are directly bonded. The structural differences affect both the thermal and spectral properties of the compounds. Migration of hmta molecules from the outer to the inner coordination sphere (especially when it results in creation of polymeric compounds) leads to increase of thermal stability of respective compounds (polymeric **2** and **4** *versus* nonpolymeric **1** and **3**). The analogous situation occurs in case of coordination sphere migration of nitrate(V) anions (**4** *versus* **3**).

Supplementary material

Tables of crystal data and structure refinement, anisotropic displacement coefficients, atomic coordinates and equivalent isotropic displacement parameters for nonhydrogen atoms, H-atom coordinates and isotropic displacement parameters, bond lengths, and interbond angles have been deposited with the Cambridge Crystallographic Data Center under No. CCDC963566, CCDC963567, CCDC963568 and CCDC963569, respectively, for **1**, **2**, **3**, and **4**.

References

[1] A. Trzesowska, R. Kruszynski. *J. Coord. Chem.*, **61**, 2167 (2008).
[2] B. Moulton, M.J. Zaworotko. *Chem. Rev.*, **101**, 1629 (2001).
[3] G. Li, C. Wang, X. Zhang. *J. Coord. Chem.*, **66**, 1107 (2013).
[4] Y. Bai, W.-L. Shang, D.-B. Dang, J.-D. Sun, H. Gao. *Spectrochim. Acta. Part A*, **72**, 407 (2009).

[5] L.-L. Li, S.-N. Wang, J. Lu, F. Cao, L.-Q. Kong, J.-M. Dou, D.-C. Li. *J. Coord. Chem.*, **66**, 306 (2013).
[6] O.M. Yaghi, G. Li, H. Li. *Nature*, **378**, 703 (1995).
[7] S.S.-Y. Chui, S.M.-F. Lo, J.P.H. Charmant, A.G. Orpen, I.D. Williams. *Science*, **283**, 1148 (1999).
[8] P.C. Srivastava, V. Singh, S. Dwivedi, T. Pujan, A.K. Bhuj, R.J. Butcher, M. Bala Murali Krishna, D. Narayana Rao. *Polyhedron*, **42**, 36 (2012).
[9] A.G.F. Shoair. *J. Coord. Chem.*, **65**, 3511 (2012).
[10] J.H. Jung, J.H. Lee, J.R. Silverman, G. John. *Chem. Soc. Rev.*, **43**, 924 (2013).
[11] F. D'Souza, E. Maligaspe, A.S.D. Sandanayaka, N.K. Subbaiyan, P.A. Karr, T. Hasobe, O. Ito. *J. Phys. Chem. A*, **144**, 10951 (2010).
[12] J.C. Garno, G. Bazzan, J.D. Batteas, C.M. Drain. *ACS Sym. Ser.*, **928**, 168 (2006).
[13] K.A. Siddiqui, G.K. Mehrotra. *J. Coord. Chem.*, **66**, 1746 (2013).
[14] M. Fujita, Y.J. Kwon, S. Washizu, K. Ogura. *J. Am. Chem. Soc.*, **116**, 1151 (1994).
[15] J. Qian, L.-P. Wang, J.-L. Tian, C.-Z. Xie, S.-P. Yan. *J. Coord. Chem.*, **65**, 122 (2012).
[16] K. Liu, W. Shi, P. Cheng. *Dalton Trans.*, 8475 (2011).
[17] S. Banerjee, M.G.B. Drew, A. Ghosh. *Polyhedron*, **22**, 2933 (2003).
[18] Q. Liu, B. Li, Z. Xu. *Transition Met. Chem.*, **27**, 786 (2002).
[19] X. Shen, N. Liu, K. Utsunomiya, L. Sun, B.-K. Jiang, X. Wang, Y.-Q. Yang, Y. Xu, K. Sakata, D.-R. Zhu. *J. Inorg. Organomet. Polym.*, **21**, 91 (2011).
[20] C.-F. Yan, C.-Y. Yue, M.-Y. Wu, L. Chen, R. Feng, F.-L. Jiang, M.-C. Hong. *Chin. J. Struct. Chem. (Hiegou Huaxue)*, **28**, 453 (2009).
[21] H.A. Habib, B. Gil-Hernandez, K. Abu-Shandi, J. Sanchiz, C. Janiak. *Polyhedron*, **29**, 2537 (2010).
[22] A.M. Kirillov. *Coord. Chem. Rev.*, **255**, 1603 (2011).
[23] T. Sieranski, R. Kruszynski. *J. Therm. Anal. Calorim.*, **109**, 141 (2012).
[24] R. Kruszynski, T. Sieranski, B. Lewinski, A. Trzesowska-Kruszynska, E. Czubacka. *Int. J. Inorg. Chem.*, Article ID 516832 (2012).
[25] A. Banerjee, P. Maiti, T. Chattopadhyay, K.S. Banu, M. Chosh, E. Suresh, E. Zangrando, D. Das. *Polyhedron*, **29**, 951 (2010).
[26] M. Vinodu, I. Goldberg. *New J. Chem.*, **28**, 1250 (2004).
[27] A. Trzesowska-Kruszynska, R. Kruszynski, M. Zalewicz, T.J. Bartczak. *J. Coord. Chem.*, **63**, 1013 (2010).
[28] M.G. Looney, D.H. Solomon. *Aust. J. Chem.*, **48**, 323 (1995).
[29] R. Kruszynski, T. Sieranski, A. Bilinska, T. Bernat, E. Czubacka. *Struct. Chem.*, **23**, 1643 (2012).
[30] T. Sieranski, R. Kruszynski. *J. Coord. Chem.*, **66**, 42 (2013).
[31] W.E. Silva, S. Alves Jr, R.F. De Farias. *J. Coord. Chem.*, **57**, 967 (2004).
[32] S.R. Batten, A.R. Harris, K.S. Murray, J.P. Smith. *Cryst. Growth Des.*, **2**, 87 (2002).
[33] W.-M. Bu, L. Ye, Y.-G. Fan. *Inorg. Chem. Commun.*, **3**, 194 (2000).
[34] N. Katsaros, J.M. Tsangaris, G.M. Tsangaris. *Monatsh. Chem.*, **114**, 27 (1983).
[35] M. Zalewicz, B. Golinski. *J. Chem. Crystallogr.*, **28**, 879 (1998).
[36] M. Zalewicz, T.J. Bartczak. *J. Cryst. Spectrosc.*, **23**, 417 (1993).
[37] S.-M. Fang, D.-L. Peng, M. Chen, L.-R. Jia, M. Hu. *J. Coord. Chem.*, **65**, 668 (2012).
[38] R. Kruszynski. *Inorg. Chim. Acta*, **371**, 111 (2011).
[39] Y.-H. Wen, Y.-Y. Chen, H.-L. Wen, X.-L. Xie, L. Wang. *J. Coord. Chem.*, **65**, 2780 (2012).
[40] X.-F. Wang, X.-Y. Yu, J.-K. Hu, H. Zhang. *J. Coord. Chem.*, **66**, 2118 (2013).
[41] J.A. Drewry, P.T. Gunning. *Coord. Chem. Rev.*, **255**, 459 (2011).
[42] K.L. Haas, K.J. Franz. *Chem. Rev.*, **109**, 4921 (2009).
[43] B. Liu, G. Yang, Y. Wang, R. Liu, L. Hou, Q. Shi. *Inorg. Chim. Acta*, **367**, 127 (2011).
[44] S.L. Xiao, Y.Q. Zhao, C.H. He, G.H. Cui. *J. Coord. Chem.*, **66**, 89 (2013).
[45] T. Matsukura, H. Tanaka. *Biochemistry*, **65**, 817 (2000).
[46] S. Trakhanov, D.I. Kreimer, S. Parkin, G. Ferro-Luzzi Ames, B. Rupp. *Protein Sci.*, **7**, 600 (1998).
[47] Y.V. Kokunov, Y. Gorbunova, G. Razgonyaeva, S.A. Kozyukhin. *Russ. J. Coord. Chem.*, **38**, 657 (2012).
[48] A. Aijaz, P. Lama, E.C. Sanudo, R. Mishra, P.K. Bharadwaj. *New J. Chem.*, **34**, 2502 (2010).
[49] F. Semerci, O.Z. Yesilel, M.S. Soylu, S. Keskin, O. Buyukgungor. *Polyhedron*, **50**, 314 (2013).
[50] M. Hakimi, K. Moeini, Z. Mardani, E. Schuh, F. Mohr. *J. Coord. Chem.*, **66**, 1129 (2013).
[51] D. Kumar, I.P.S. Kapoor, G. Singh, N. Goel, U.P. Singh. *Solid State Sci.*, **14**, 495 (2012).
[52] G. Singh, B.P. Baranwal, I.P.S. Kapoor, D. Kumar, C.P. Singh, R. Fröhlich. *J. Therm. Anal. Calorim.*, **91**, 971 (2008).
[53] B. Viossat, P. Khodadad, N. Rodier. *Acta Crystallogr.*, **B38**, 3075 (1982).
[54] *X-RED (Version 1.18)*, STOE & Cie GmbH, Darmstadt, Germany (1999).
[55] G.M. Sheldrick. *Acta Crystallogr.*, **A46**, 467 (1990).
[56] G.M. Sheldrick. *SHELXL97. Program for the Solution and Refinement of Crystal Structures*, University of Gottingen, Germany (1997).
[57] G.M. Sheldrick. *SHELXTL: Release 4.1 for Siemens Crystallographic Research Systems*, University of Gottingen, Germany (1990).

[58] F.J. Welcher. *Analityczne Zastosowanie Kwasu Wersenowego (The Analytical Uses of Ethylenediaminetetraacetic Acid)*, WNT, Warsaw, Poland (1963).
[59] *Data Processing Module (Version 1.4)*, Copyright 1994–1998 SETARAM – FRANCE.
[60] *Powder Diffraction File International Center of Diffraction Data*, 12 Campus Boulevard, Newton Square, PA, USA (2003).
[61] F.H. Allen. *Acta Crystallogr.*, **B58**, 380 (2002).
[62] T. Han. *International Tables for Crystallography*, Vol. A, p. 177, The International Union of Crystallography, Dordrecht, Holland (1983).
[63] D.L. Smith. In *Progress in Inorganic Chemistry*, S.J. Lippard (Ed.), Vol. 23, pp. 1–65, John Wiley, New York (1977).
[64] M. Terpstra, M. Craven, R.F. Stewart. *Acta Crystallogr.*, **A49**, 685 (1993).
[65] W.H. Zachariasen. *J. Less-Common Met.*, **62**, 1 (1978).
[66] I.D. Brown. *Acta Crystallogr.*, **B53**, 381 (1997).
[67] I.D. Brown. *Acta Crystallogr.*, **B48**, 553 (1992).
[68] M. O'Keeffe, N.E. Brese. *Acta Crystallogr.*, **B47**, 192 (1997).
[69] A. Trzesowska, R. Kruszynski, T.J. Bartczak. *Acta Crystallogr.*, **B60**, 174 (2004).
[70] A. Trzesowska, R. Kruszynski, T.J. Bartczak. *Acta Crystallogr.*, **B61**, 429 (2005).
[71] M.C. Etter, J.C. MacDonald, J. Bernstein. *Acta Crystallogr.*, **B46**, 256 (1990).
[72] L. Shimoni, J.P. Glusker, C.W.J. Bock. *Phys. Chem.*, **100**, 2957 (1996).
[73] J. Bernstein, L. Shimoni, R.E. Davis, N.L. Chang. *Angew. Chem. Int. Ed. Engl.*, **34**, 1555 (1995).
[74] R. Kruszynski, T. Sieranski. *Cent. Eur. J. Chem.*, **9**, 94 (2011).
[75] J. Straszko, M. Olszak-Humienik, J. Mozejko. *Thermochim. Acta*, **292**, 145 (1997).
[76] A. Basinski, Z. Bankowski, B. Bobranski, B. Bochwic, J. Bohm, H. Calus, H. Dokowska, A. Dorabialska, W. Gajewski, J. Galecki, A. Hulanicki, M. Janczak, Z. Jonscherowa, W. Kemula, Z. Lada, Z. Mars, J. Michalski, J. Minczewski, I. Pakosz, W. Polaczkowa, K. Tuszynski, J. Waclawik, W. Wolfram, J. Wolinski, T. Zamoyski, J. Zienkowicz. *Kalendarz Chemiczny*, Państwowe Wydawnictwa Techniczne, Warszawa [Handbook of Chemistry, National Technological Publishing House, Warsaw (1954)] (1954).
[77] K.T. Wojciechowski, A. Malecki. *Thermochim. Acta*, **331**, 73 (1999).
[78] B. Malecka, R. Gajerski, A. Malecki, M. Wierzbicka, P. Olszewski. *Thermochim. Acta*, **404**, 125 (2003).
[79] K.H. Stern. *J. Phys. Chem. Ref. Data*, **1**, 747 (1972).
[80] M.P. Bernstein, S.A. Sandford, L.J. Allamandola, S. Chang. *J. Phys. Chem.*, **98**, 12206 (1994).
[81] J.O. Jensen. *Spectrochim. Acta*, **A58**, 1347 (2002).
[82] J.K. Saha, J. Podder. *J. Bangladesh Acad. Sci.*, **35**, 203 (2011).
[83] G. Rajadurai, A. Puhal Raj, S. Pari. *Arch. Appl. Sci. Res.*, **5**, 247 (2013).
[84] C.C. Addison, B.M. Gatehouse. *J. Chem. Soc.*, 613 (1960).
[85] R.E. Hester, C.W.J. Scaife. *J. Chem. Phys.*, **47**, 5253 (1967).
[86] J.T. Kloprogge, D. Wharton, L. Hickey, R.L. Frost. *Am. Mineral.*, **87**, 623 (2002).
[87] J.T. Kloprogge, R.D. Schuiling, Z. Ding, L. Hickey, D. Wharton, R.L. Frost. *Vib. Spectrosc.*, **28**, 209 (2002).